

Jonathan Jones et al. *Editors*

# Advanced GNSS Tropospheric Products for Monitoring Severe Weather Events and Climate

COST Action ES1206 Final  
Action Dissemination Report



# Advanced GNSS Tropospheric Products for Monitoring Severe Weather Events and Climate

Jonathan Jones • Guergana Guerova  
Jan Douša • Galina Dick • Siebren de Haan  
Eric Pottiaux • Olivier Bock • Rosa Pacione  
Roeland van Malderen

Editors

# Advanced GNSS Tropospheric Products for Monitoring Severe Weather Events and Climate

COST Action ES1206 Final Action  
Dissemination Report



Funded by the Horizon 2020 Framework Programme  
of the European Union

*Editors*

Jonathan Jones  
Met Office  
Exeter, UK

Jan Douša  
Geodetic Observatory Pecný, RIGTC  
Ondřejov, Czech Republic

Siebren de Haan  
Royal Netherlands Meteorological Institute  
De Bilt, The Netherlands

Olivier Bock  
IGN Institut national de l'information  
géographique et forestière  
Paris, France

Roeland van Malderen  
Royal Meteorological Institute (RMI)  
Brussels, Belgium

Guergana Guerova  
Physics Faculty, Department of Meteorology and  
Geophysics  
Sofia University "St. Kliment Ohridski"  
Sofia, Bulgaria

Galina Dick  
GFZ German Research Centre for Geosciences  
Helmholtz Centre Potsdam  
Potsdam, Germany

Eric Pottiaux  
Royal Observatory of Belgium  
Brussels, Belgium

Rosa Pacione  
e-GEOS/Centro di Geodesia Spaziale-Agenzia  
Spaziale Italiana  
Matera, MT, Italy

This publication is based upon work from COST Action ES1206: Advanced Global Navigation Satellite Systems tropospheric products for monitoring severe weather events and climate, supported by COST (European Cooperation in Science and Technology). [www.cost.eu](http://www.cost.eu)

COST (European Cooperation in Science and Technology) is a funding agency for research and innovation networks. Our Actions help connect research initiatives across Europe and enable scientists to grow their ideas by sharing them with their peers. This boosts their research, career and innovation.

ISBN 978-3-030-13900-1

ISBN 978-3-030-13901-8 (eBook)

<https://doi.org/10.1007/978-3-030-13901-8>

© Springer Nature Switzerland AG 2020

This work is subject to copyright. All rights are reserved by the Publisher, whether the whole or part of the material is concerned, specifically the rights of translation, reprinting, reuse of illustrations, recitation, broadcasting, reproduction on microfilms or in any other physical way, and transmission or information storage and retrieval, electronic adaptation, computer software, or by similar or dissimilar methodology now known or hereafter developed.

The use of general descriptive names, registered names, trademarks, service marks, etc. in this publication does not imply, even in the absence of a specific statement, that such names are exempt from the relevant protective laws and regulations and therefore free for general use.

The publisher, the authors, and the editors are safe to assume that the advice and information in this book are believed to be true and accurate at the date of publication. Neither the publisher nor the authors or the editors give a warranty, express or implied, with respect to the material contained herein or for any errors or omissions that may have been made. The publisher remains neutral with regard to jurisdictional claims in published maps and institutional affiliations.

Cover illustration: GNSS severe weather schematic, Sofia, Bulgaria, March 2018, Courtesy of Dr Tzvetan Simeonov, Sofia University.

This Springer imprint is published by the registered company Springer Nature Switzerland AG.  
The registered company address is: Gewerbestrasse 11, 6330 Cham, Switzerland

# Preface

This book presents the state of the art of atmospheric remote sensing using GNSS signal delays in Europe, conducted within COST Action ES1206 ‘Advanced Global Navigation Satellite Systems Tropospheric Products for Monitoring Severe Weather Events and Climate’ (GNSS4SWEC, 2013–2017). It is well-suited for graduate students in the fields of geodesy and meteorology but also for a broader audience concerned with environmental remote sensing. The Action was initially suggested in mid-2011 during informal discussions at the third International Colloquium on Scientific and Fundamental Aspects of the Galileo Program, Copenhagen, and formally began at the kick-off meeting in Brussels, May 2013. As stated in the GNSS4SWEC Memorandum of Understanding (MoU), the main objective of the Action is to ‘enhance existing and develop new, ground-based multi-Global Navigation Satellite Systems (GNSS) tropospheric products, assess their usefulness in severe weather forecasting and climate monitoring, and improve GNSS accuracy through enhanced atmospheric modelling’.

A previous COST Action (716) established and to some degree matured GNSS-meteorology in Western Europe, but its establishment across the whole of Europe was only achieved by GNSS4SWEC. Over 160 participants from 32 COST countries, 1 near-neighbour country and 4 international partner countries contributed to the work of the three Action working groups. GNSS4SWEC helped introduce GNSS meteorology to 11 European countries and in the establishment of 7 new GNSS Analysis Centres in previously data-sparse regions, e.g. south-east Europe and the Baltic region. Production and exploitation of next-generation GNSS tropospheric products with high spatio-temporal resolution for use in operational numerical weather prediction (e.g. within E-GVAP) are a major step forward (Chap. 3). The GNSS potential in nowcasting severe weather has been demonstrated using case studies, and its implementation in pre-operational tools is evolving at European National Meteorological Services (Chap. 4). The new field of GNSS climatology

was established as a result of GNSS4SWEC (Chap. 5). Chapters 6 and 7 present the national status reports and the outcomes of COST-funded short-term scientific missions (STSMs).

Enjoy reading!

Met Office, Exeter, United Kingdom	Jonathan Jones
Sofia University “St. Kliment Ohridski”, Sofia, Bulgaria	Guergana Guerova
Geodetic Observatory Pecný, RIGTC, Ondřejov, Czech Republic	Jan Douša
GFZ German Research Centre for Geosciences, Potsdam, Germany	Galina Dick
Royal Netherlands Meteorological Institute, De Bilt, The Netherlands	Siebren de Haan
Royal Observatory of Belgium, Brussels, Belgium	Eric Pottiaux
IGN Institut national de l'information géographique et forestière, Paris, France	Olivier Bock
e-GEOS/Centro di Geodesia Spaziale-Agenzia Spaziale Italiana, Matera, Italy	Rosa Pacione
Royal Meteorological Institute (RMI), Brussels, Belgium	Roeland van Malderen

May 2019

# Acknowledgement

Firstly, we would like to thank the COST Association in Brussels for the faith and vision to fund this COST Action and for their invaluable work encouraging and facilitating science and technology across Europe. In particular, we would like to thank Dr. Deniz Karaca and Ms. Tania Gonzalez-Ovin for the essential scientific and administrative support they have provided over the course of the Action.

We would like to thank all the GNSS network operators and data providers, as well as the IGS and EUREF – without which there would be no data for such scientific study. In addition, we would like to recognise and thank a number of European and national research projects whose support has been fundamental.

We would like to thank the support from all the participants' institutions (Appendix B), and special thanks must go to those people and institutions who have been involved in hosting meetings and workshops (Appendix A).

Finally, we would like to thank all of the participants of GNSS4SWEC; without your enthusiastic participation, none of this would have been possible. Particular thanks to a number of people who made significant contributions to coordination:

- Michal Kačmařík for coordinating and reporting on the WG1 benchmark campaign and slant delays intercomparisons and the help with the Final Report
- Hugues Brenot for coordinating and reporting on the WG1 sub-group for asymmetry modelling
- Florian Zus for coordinating and reporting on the WG1 sub-group for NWP tropospheric parameter modelling
- Pavel Václavovic for organising the WG1 real-time demonstration campaign and for organising the WG1 PPP sub-group
- Norman Teferle for coordinating the WG1 sub-group for ultra-fast products
- Zhiguo Deng for reporting on WG1 sub-group for multi-GNSS development
- Karolina Szafranek for reporting on WG1 sub-group new ACs and networks
- Wolfgang Söhne for support with completing the WG1 Final Report
- Jan Kaplon, Gregor Möller, Radmila Brožková and Pavla Skřivánková for support with the WG1 benchmark dataset

- Witold Rohm for organising the WG2 tomography sub-group
- Gemma Halloran for organising the WG2 numerical nowcasting and NWP assimilation sub-group
- Furqan Ahmed for coordinating and reporting on the WG3 ZTD datasets sub-group
- Anna Klos for coordinating and reporting on the WG3 homogenisation sub-group

May 2019

The Editors

# Abstract

The path delay between a GNSS satellite and a ground-based GNSS receiver depends, after elimination of ionospheric effects using a combination of two GNSS frequencies, on the integral effect of the densities of dry air and water vapour along the signal path. The total delay in the signal from each satellite is known as the slant delay as the path is most likely to be non-azimuthal. The slant paths are then transferred into the vertical (or zenith) by an elevation-dependent mapping function, and this new parameter is known as the zenith total delay or ZTD. ZTD gives a measure for the integrated atmospheric condition and is now widely accepted as a standard product from a network of dual-frequency GNSS receivers. With further calculation, taking into account surface pressure and temperature, we can then convert a portion of the ZTD into an estimate of the integrated water vapour (IWV) content of the atmosphere.

As IWV may potentially change rapidly on very short timescales, it is the speed as well as accuracy at which IWV can be calculated which is of critical importance to short-term meteorological forecasting or ‘nowcasting’. Often, rapid changes in IWV are associated with high humidity conditions linked to extreme weather events such as thunderstorms. Extreme weather events such as these are typically difficult to predict and track under traditional operational meteorological observing systems, and as they have the potential to cause great damage and risk to life, it is in the interests to both the public and national meteorological services to significantly improve nowcasting wherever possible. As such, the requirement for dense near real-time GNSS networks for meteorological applications becomes apparent. Furthermore, water vapour is one of the most important constituents of the atmosphere as moisture and latent heat are primarily transmitted through the water vapour phase. As such, water vapour is one of the most important greenhouse gases typically accounting for 60–70 % of atmospheric warming, and thus, accurate, long-term monitoring of atmospheric water vapour is of great importance to climatological research.

COST Action ES1206: Advanced Global Navigation Satellite Systems Tropospheric Products for Monitoring Severe Weather Events and Climate

(GNSS4SWEC) addresses new and improved capabilities from concurrent developments in both the GNSS and meteorological communities. For the first time, the synergy of three operational GNSS systems (GPS, GLONASS and Galileo) is used to develop new, more advanced tropospheric products, exploiting the full potential of multi-GNSS water vapour estimates on a wide range of temporal and spatial scales, from real-time monitoring and forecasting of severe weather to climate research.

The Action also promotes the use of meteorological data as an input to GNSS positioning, navigation and timing services and aims to stimulate knowledge transfer and data sharing throughout Europe.

# Contents

<b>1</b>	<b>Scientific Background . . . . .</b>	<b>1</b>
1.1	Atmospheric Water Vapour . . . . .	1
1.2	Global Navigation Satellite Systems (GNSS) . . . . .	6
1.2.1	GPS Basics . . . . .	6
1.2.2	Delay in the Neutral Atmosphere . . . . .	9
1.2.3	Zenith Delay Estimates . . . . .	11
1.2.4	Derivation of IWV from ZTD . . . . .	12
	References . . . . .	14
<b>2</b>	<b>General Background . . . . .</b>	<b>17</b>
2.1	Introduction . . . . .	18
2.2	The State-of-the-Art at the Start of the Action (E-GVAP) . . . . .	19
2.3	Reasons for the Action . . . . .	23
2.4	Objectives . . . . .	24
2.5	Impacts and Benefits . . . . .	25
2.5.1	Societal Benefits . . . . .	25
2.5.2	Scientific Benefits . . . . .	25
2.5.3	Technological Benefits . . . . .	26
2.5.4	Economic Benefits . . . . .	26
2.5.5	Target Groups and End-Users . . . . .	26
2.6	Scientific Programme . . . . .	27
2.7	Scientific Work Plans . . . . .	28
2.7.1	Working Group 1: Advanced GNSS Processing Techniques . . . . .	28
2.7.2	Working Group 2: Use of GNSS Tropospheric Products for High-Resolution, Rapid-Update NWP and Severe Weather Forecasting . . . . .	29
2.7.3	Working Group 3: Use of GNSS Tropospheric Products for Climate Monitoring . . . . .	30

<b>3 Advanced GNSS Processing Techniques (Working Group 1) . . . . .</b>	<b>33</b>
3.1 Introduction . . . . .	36
3.2 Campaigns for Development of Advanced Tropospheric Products . . . . .	37
3.2.1 Benchmark Campaign – Common Data Set for New Product Development and Validation . . . . .	37
3.2.2 GNSS Real-Time PPP Demonstration Campaign . . . . .	45
3.3 Tropospheric Asymmetry Monitoring and Advantage of Multi-GNSS . . . . .	48
3.3.1 Concept of Tropospheric Gradients . . . . .	49
3.3.2 Global Validity and Behaviour of Tropospheric Gradients Estimated by GPS . . . . .	53
3.3.3 Monitoring of Severe Weather from Wet Gradients, Residuals and Slants . . . . .	55
3.3.4 Indicator of Tropospheric Activity Based on the Disruption of GNSS Signals . . . . .	61
3.3.5 Validation of Slant Tropospheric Delays . . . . .	71
3.3.6 Information Content in Post-fit Residuals, PPP vs DD Approach . . . . .	84
3.3.7 Tropospheric Parameters from Multi-GNSS Analysis . . . . .	86
3.3.8 Multi-GNSS Solutions and Products . . . . .	91
3.4 PPP and Ultra-Fast GNSS Tropospheric Products . . . . .	92
3.4.1 Real-Time Data and Product Dissemination . . . . .	94
3.4.2 BKG Real-Time Analysis Development and Contribution . . . . .	96
3.4.3 Assessment of IGS RTS Orbits and Clock Corrections and GOP Real-Time Tropospheric Products . . . . .	101
3.4.4 Real-Time Product Development and Evaluation at ROB . . . . .	106
3.4.5 GFZ Real-Time Product Development and Assessment in RT Analysis . . . . .	113
3.4.6 Contribution to RT Demonstration Campaign from ULX . . . . .	114
3.4.7 New Adaptable Strategy for RT and NRT Troposphere Monitoring . . . . .	119
3.4.8 Optimum Stochastic Modeling for GNSS Tropospheric Delay Estimation in Real-Time . . . . .	124
3.5 Exploiting NWM-Based Products for Precise Positioning . . . . .	126
3.5.1 Tropospheric Parameters from Numerical Weather Models . . . . .	127
3.5.2 The Impact of Global and Regional Climatology on the Performance of Tropospheric Blind Models . . . . .	133
3.5.3 Refined Discrete and Empirical Troposphere Mapping Functions VMF3 and GPT3 . . . . .	135

3.5.4	The Impact of NWM Forecast Length on ZTDs . . . . .	136
3.5.5	Dual-Layer Tropospheric Correction Model Combining Data from GNSS and NWM . . . . .	138
3.5.6	Tropospheric Refractivity and Zenith Path Delays from Least-Squares Collocation of Meteorological and GNSS Data . . . . .	142
3.5.7	Improving Precise Point Positioning with Numerical Weather Models . . . . .	144
3.5.8	Using External Tropospheric Corrections to Improve GNSS Positioning of Hot-Air Balloon . . . . .	145
3.5.9	Real-Time PPP Augmented with High-Resolution NWM Model Data . . . . .	149
3.5.10	Validation and Implementation of Direct Tropospheric Delay Estimation for Precise Real-Time Positioning . . . . .	150
3.6	GNSS Data Reprocessing for Climate . . . . .	158
3.6.1	EUREF Repro2 Contribution of Swisstopo . . . . .	158
3.6.2	EUREF Repro2 Assessment of GOP Processing Variants . . . . .	163
3.6.3	CORDEX.be Reprocessing . . . . .	167
3.6.4	GRUAN Reprocessing . . . . .	169
3.6.5	GFZ TIGA Reprocessing . . . . .	170
3.6.6	ULX TIGA Reprocessing . . . . .	172
3.7	New Analysis Centres, Networks and Solutions . . . . .	174
3.7.1	Trop-NET System for Collaborative Ground-Based GNSS Meteorology . . . . .	174
3.7.2	Sofia University GNSS Analysis Centre (SUGAC): First Processing Campaign . . . . .	178
3.7.3	TU Wien Near Real-Time GNSS Analysis Centre in Austria (TUW AC): First Processing Results . . . . .	182
3.7.4	New Operational Solutions from ROB in Support to Global NWP Models and Rapid-Update Numerical Nowcasting . . . . .	183
3.7.5	New Methods to User GNSS Vapor Estimates for Meteorology (NUVEM) . . . . .	185
3.7.6	Near Real-Time GNSS Processing at ASI/CGS, Italy . . . . .	187
3.7.7	New Analysis Centre (AUTh) and National Observatory of Athens (NOA) . . . . .	189
3.7.8	New Analysis Centre in Iceland, Icelandic Meteorological Office (IMO) . . . . .	193
3.7.9	New Analysis Centre in Hungary (BUTE) . . . . .	194
	References . . . . .	194

<b>4 Use of GNSS Tropospheric Products for High-Resolution, Rapid-Update NWP and Severe Weather Forecasting (Working Group 2) . . . . .</b>	203
4.1 Introduction . . . . .	205
4.2 Non-numerical Nowcasting . . . . .	206
4.2.1 Investigation of Fog in Bulgaria Using GNSS Tropospheric Products . . . . .	206
4.2.2 WRF Model Evaluation with GNSS IWV for Intense Precipitation Cases in Bulgaria . . . . .	210
4.2.3 Case Study of Foehn in Sofia with GNSS Tropospheric Products . . . . .	217
4.2.4 A GNSS-Based Nowcasting Toolbox for Severe Weather in Belgium . . . . .	221
4.3 Numerical Nowcasting and NWP Data Assimilation . . . . .	235
4.3.1 HARMONIE-AROME Group . . . . .	235
4.3.2 Assimilation of E-GVAP ZTD Data into the WRF Model . . . . .	236
4.3.3 Improvement of Forecast Skill of the GLAMEPS Model . . . . .	238
4.3.4 Slant Total Delay Assimilation in COSMO-DE: First Results . . . . .	242
4.3.5 Data Assimilation Experiments with GNSS ZTD in AROME 3DVAR . . . . .	247
4.4 Tomography . . . . .	249
4.4.1 Nowcasting Using Tomography . . . . .	250
4.4.2 Requirements for Assimilation of Tomography Results . . . . .	250
4.4.3 Assimilation of Relative Humidity . . . . .	251
4.4.4 Assimilation of Temperature and Specific Humidity . . . . .	252
4.4.5 Assimilation of Wet Refractivity . . . . .	255
4.4.6 Conclusions . . . . .	257
4.5 Benchmark and Case Study Databases at the U.K. Met Office . . . . .	259
4.6 ZTD to IWV Conversion . . . . .	260
References . . . . .	262
<b>5 Use of GNSS Tropospheric Products for Climate Monitoring (Working Group 3) . . . . .</b>	267
5.1 Introduction . . . . .	270
5.1.1 Motivation . . . . .	270
5.2 Available Reprocessed ZTD and IWV Datasets . . . . .	273
5.2.1 Inventory of Available Reprocessed ZTD Datasets . . . . .	273
5.2.2 IGS Repro1 as First Reference GNSS IWV Dataset . . . . .	275
5.2.3 EPN Repro2 GNSS Reprocessing Campaign . . . . .	279
5.2.4 VLBI Reprocessing Campaign . . . . .	281
5.2.5 DORIS Reprocessing Campaign . . . . .	282

5.3	Sensitivity Studies on GNSS Processing Options . . . . .	284
5.3.1	An Overview of the GNSS Data Processing Strategies . . . . .	284
5.3.2	Software Agreement . . . . .	285
5.3.3	PPP vs. DD Processing Modes . . . . .	287
5.3.4	Baseline Strategy in DD Processing . . . . .	290
5.3.5	Mapping Functions . . . . .	291
5.3.6	Trends in the IWV Estimated from Ground-Based GPS Data: Sensitivity to the Elevation Cutoff Angle . . . . .	296
5.3.7	Improving Stochastic Tropospheric Model for Better Estimates During Extreme Weather Events . . . . .	297
5.3.8	Multi-GNSS Data Processing . . . . .	301
5.3.9	Impact of IGS Type Mean and EPN Individual Antenna Calibration Models . . . . .	302
5.3.10	Impact of Non-Tidal Atmospheric Loading Models . . . . .	303
5.3.11	Using Estimated Horizontal Gradients as a Tool for Assessment of GNSS Data Quality . . . . .	304
5.3.12	Conclusions and Recommendations on Processing Options . . . . .	312
5.4	Standardisation of ZTD Screening and IWV Conversion . . . . .	314
5.4.1	ZTD Screening . . . . .	314
5.4.2	ZTD to IWV Conversion . . . . .	318
5.4.3	The Uncertainty of the Atmospheric Integrated Water Vapour Estimated from GNSS Observations . . . . .	324
5.5	ZTD/IWV Homogenisation . . . . .	326
5.5.1	Introduction . . . . .	327
5.5.2	Methodology . . . . .	328
5.5.3	Assessment of the Homogeneity of ERA-Interim . . . . .	330
5.5.4	Synthetic Gataset Generation . . . . .	331
5.5.5	Involved Homogenization Algorithms . . . . .	332
5.5.6	Assessment of the Performance of the Tools on the Synthetic Datasets . . . . .	335
5.5.7	Conclusions and Outlook . . . . .	337
5.6	IWV Intercomparisons . . . . .	339
5.6.1	A Literature Overview . . . . .	339
5.6.2	A Comparison of Precipitable Water Vapour Products Over the Iberian Peninsula . . . . .	347
5.6.3	Comparing Precipitable Water from Remote Sensing and Space Geodetic Techniques with Numerical Weather Models . . . . .	351
5.6.4	Inter-Comparison Analysis of Tropospheric Parameters Derived from GPS and RAOB Data Observed in Sodankylä, Finland . . . . .	355

<b>5.7</b>	<b>IWV Trends &amp; Variability from GNSS Data and Atmospheric Models . . . . .</b>	358
5.7.1	Analysis of IWV Trends and Variability from GNSS and Re-Analyses . . . . .	358
5.7.2	Analysis of IWV Trends and Variability from GNSS and Satellite Data . . . . .	364
5.7.3	Evaluation of IWV Diurnal Variation in Regional Climate Models using GPS . . . . .	369
5.7.4	Validation of the Regional Climate Model ALARO-SURFEX by EPN Repro2 . . . . .	373
5.7.5	Evaluation of IWV Trends and Variability in a Global Climate Model . . . . .	374
5.7.6	Anomalies of Hydrological Cycle Components During the 2007 Heat Wave in Bulgaria . . . . .	381
<b>5.8</b>	<b>Database, Formats and Dissemination . . . . .</b>	384
5.8.1	GOP-TropDB – Comparison Tropospheric Database . .	384
5.8.2	Tropo SINEX Format . . . . .	389
	<b>References . . . . .</b>	390
<b>6</b>	<b>National Status Reports . . . . .</b>	403
<b>6.1</b>	<b>COST Countries . . . . .</b>	407
6.1.1	Austria . . . . .	407
6.1.2	Belgium . . . . .	408
6.1.3	Bulgaria . . . . .	410
6.1.4	Cyprus . . . . .	412
6.1.5	Czech Republic . . . . .	414
6.1.6	Denmark . . . . .	417
6.1.7	Estonia . . . . .	418
6.1.8	Finland . . . . .	419
6.1.9	France . . . . .	421
6.1.10	Germany . . . . .	422
6.1.11	Greece . . . . .	427
6.1.12	Hungary . . . . .	427
6.1.13	Iceland . . . . .	429
6.1.14	Israel . . . . .	431
6.1.15	Italy . . . . .	432
6.1.16	Lithuania . . . . .	435
6.1.17	Luxembourg . . . . .	436
6.1.18	Poland . . . . .	439
6.1.19	Portugal . . . . .	442
6.1.20	Slovakia . . . . .	443
6.1.21	Spain . . . . .	446
6.1.22	Sweden . . . . .	449
6.1.23	Switzerland . . . . .	453
6.1.24	Turkey . . . . .	457

<b>Contents</b>	xvii
6.1.25 United Kingdom . . . . .	458
<b>6.2 COST International Partner Countries . . . . .</b>	<b>463</b>
6.2.1 Hong Kong . . . . .	463
6.2.2 Australia . . . . .	469
6.2.3 Canada . . . . .	473
References . . . . .	474
<b>7 STSM Reports . . . . .</b>	<b>483</b>
References . . . . .	507
<b>Appendices . . . . .</b>	<b>509</b>
References . . . . .	563

# Glossary

3D-Var	Three-dimensional variational data assimilation system
4D-Var	Four-dimensional variational data assimilation system
AC	Analysis centre
ARP	Antenna reference point
ASI	Agenzia Spaziale Italiana (Italian Space Agency)
BKG	Bundesamt für Kartographie und Geodäsie, Germany
BNC	BKG Ntrip Client
BSW	Bernese Software
BUFR	Binary universal format for the representation of data (WMO)
CFSR	Climate Forecast System Reanalysis
CODE	Centre for Orbit Determination in Europe
CORDEX	Coordinated Downscaling Experiment
CORS	Continuously Operating (GNSS) Reference Stations
COST	Cooperation in the Field of Scientific and Technical Research
COST716	COST Action 716: Exploitation of Ground-Based GPS for Operational Numerical Weather Prediction and Climate Applications
DD	Double-difference method of GNSS processing
DMI	Danish Meteorological Institute
DORIS	Doppler Orbitography and Radiopositioning Integrated by Satellite
DWD	Deutscher Wetterdienst (the German National Meteorological Agency)
EC	European Community
ECMWF	European Centre for Medium Range Weather Forecasting
E-GVAP	The EIG EUMETNET GNSS Water Vapour Programme
EPN	EUREF Permanent Network
EPOS	GFZ GNSS processing software package
ERA-Clim	European Reanalysis of Global Climate Observations
ERA-Interim	ECMWF global atmospheric reanalysis
ERP	Earth rotation parameter

ESA	The European Space Agency
ETRS	European Terrestrial Reference System
EUPOS	The European Position Determination System
EUREF	IAG sub-commission for regional reference frames European Reference Frame
EUMETNET	European Meteorological Network FES2004
	Finite Element Solution 2004 (OTL model)
FTP	File Transfer Protocol (under TCP/IP)
Galileo	The European GNSS
GAMIT	GPS analysis software package from MIT and SIO
GCOS	WMO Global Climate Observing System
GEOSS	Global Earth Observation System of Systems
GFZ	GFZ German Research Centre for Geosciences
GIPSY-OASIS	GPS Inferred Positioning System Orbit Analysis Simulation Software
GLONASS	Globalnaya navigatsionnaya sputnikovaya sistema (the Russian GNSS system)
GMES	<i>Global Monitoring for Environment and Security</i>
GMF	Global mapping function
GNSS	Global navigation satellite system
GOME-2	<i>Global Ozone Monitoring Experiment-2</i>
GOP	Geodetic Observatory Pecny, Czech Republic
GPS	The NAVSTAR Global Positioning System (US GNSS)
GPT	Global pressure and temperature model
GRD	Tropospheric gradient
GTS	Global Telecommunication System
HIRLAM	High Resolution Limited Area Model
IAG	International Association of Geodesy
IASI	Infrared atmospheric sounding interferometer
IERS	International Earth Rotation and Reference Systems Service
IF DD	Ionosphere-free double difference
IGS	International GNSS Service
IGU	IGS ultra rapid products
IPCC AR5	Fifth Assessment Report of the Intergovernmental Panel on Climate Change
ITRF	International Terrestrial Reference Frame
IWV	Integrated water vapour
KNMI	Koninklijk Nederlands Meteorologisch Instituut
MC	Management Committee (of the Action)
MERRA	Modern-Era Retrospective analysis for Research and Applications
MIT	Massachusetts Institute of Technology
MOPS	Moisture observation pre-processing system
MoU	Memorandum of understanding

MSL	Mean sea level
NCEP	National Center for Environmental Prediction
NGAA	The Nordic GNSS Analysis Centre
NMHS	National Meteorological and Hydrological Services
NRT	Near real time
NTRIP	Networked transport of RTCM via Internet Protocol
NWM	Numerical weather model
NWP	Numerical weather prediction
OTL	Ocean tide loading
PCO	Phase centre offset
PCV	Antenna phase centre variation
PPP	Precise point positioning method of GNSS processing
PWV	Precipitable water vapour
RAOBS	Radiosonde observations
RINEX	Receiver independent exchange format
RMS	Root mean square
RO	Radio occultation
RTK	Real-time kinematic
RTS	Real-time service (of the IGS)
SCIAMACHY	Scanning Imaging Absorption Spectrometer for Atmospheric Chartography
SIO	Scripps Institution of Oceanography
SIWV	Slant integrated water vapour
SSM/I	Special Sensor Microwave Imager
SSMIS	Special Sensor Microwave Imager Sounder
SSR	State-space representation
STD	Slant total delay
StDev	Standard deviation
TIGA	The IGS Tide Gauge Benchmark Monitoring
TOUGH	Targeting Optimal Use of GPS Humidity Measurements in Meteorology
UCAR	University Consortium for Atmospheric Research
ULX	University of Luxembourg
UM	Unified Model
UTC	Universal time co-ordinated
VLBI	Very long baseline interferometry
VMF	Vienna Mapping Function
WG	Working group
WMO	World Meteorological Organization
WVR	Water vapour radiometer
ZHD	Zenith hydrostatic delay
ZTD	Zenith total delay
ZWD	Zenith Wet Delay

# Chapter 1

## Scientific Background



J. Jones

**Abstract** This chapter covers the fundamental science behind GNSS-meteorology. Firstly, atmospheric water vapour and its role in meteorological and climate systems is covered. The Chapter then provides an overview of GNSS; how they fundamentally operate, how the atmosphere affects GNSS signals (and in particular, GNSS signal delays due to the neutral atmosphere), the conversion of atmospheric delays to integrated water vapour and the application of both signal delays and water vapour to modern meteorological observing systems.

### 1.1 Atmospheric Water Vapour

Water vapour is one of the most significant constituents of the atmosphere since it is the means by which moisture and energy (as latent heat) are transported through the troposphere and lower stratosphere. Aside from the role of water vapour in balancing the atmospheric heat budget, water vapour is obviously the source of precipitation. In any vertical column of air, the amount of water vapour provides operational meteorologists with a value of the maximum potential precipitation which could be retrieved from that column of air in optimal conditions. Also, as atmospheric water vapour is highly variable both temporally and spatially, it is a potential source of inaccuracy to the geodetic community, hence, accurate observations of atmospheric water vapour result in more accurate GNSS derived coordinates.

Although the actual amount of atmospheric water vapour is relatively low (~1%), the effect it has on the meteorology is very strong. It has the ability to cause temperature anomalies both large and small and, as mentioned, is also the main mechanism for atmospheric latent heat exchange. Furthermore, when looking at

---

Parts in this chapter are reprinted with kind permission from Jones (2010)

J. Jones (✉)  
Met Office, Exeter, UK  
e-mail: [jonathan.jones@metoffice.gov.uk](mailto:jonathan.jones@metoffice.gov.uk)

water vapour's role in the climate system, numerous scientific studies have determined that around 70% of atmospheric warming is attributable to atmospheric water vapour acting as a greenhouse gas (Houghton et al. 2001; Philipona et al. 2005).

In terms of definitions, water vapour is defined as the amount of water in gas phase (in grams per cubic metre) of air. Water vapour mixing ratio in a volume of air is the ratio of mass of water vapour and the mass of dry air. Specific humidity is the amount of water in gas phase (measured in grams in a total air volume with a mass of 1 kg). A commonly used parameter is relative humidity. Relative humidity is the ratio of the actual water vapour pressure in the air to that of the saturation (or equilibrium) water vapour pressure. Above the water vapour saturation pressure, at 100% relative humidity, any additional water vapour will condensate. The saturation pressure increases strongly with temperature, hence warm air can contain much more water vapour than cold air. Formation of clouds and precipitation is normally associated with lifting of air to levels with lower temperatures, where the air becomes over-saturated resulting in condensation.

Another way to express the water vapour content of an air parcel, is to combine all the water vapour in the vertically integrated total in any one column of air. The most commonly used terms in this case are Integrated Water Vapour (IWV) and Precipitable Water Vapour (PWV). Both terms represent the absolute total amount of water in the vertical column of air which could, hypothetically precipitate out with units of  $\text{kg/m}^2$ . The term of Integrated Water Vapour, or IWV, with units of  $\text{kg/m}^2$  will generally be used in this report as is the standard convention in Europe. Also the unit, unlike the unit of mm which is commonly used for PWV, avoids any confusion with the units used in atmospheric delay, which are units of length. The actual amount is exactly the same, as 1 kg of water spread out over 1  $\text{m}^2$  would be exactly 1 mm in height.

It is important to remember that IWV is a cumulative total amount of water vapour, in principle all the way from the ground based GNSS antenna to the GNSS satellite at an altitude of around 20,000 km depending on GNSS constellation. However, water vapour is by no means distributed evenly in the vertical. The vast majority of the water vapour is limited to the warmest, bottom most portion of the lowest part of the atmosphere known as the troposphere, see Figs. 1.1 and 1.2.

In reality, the vast majority of all atmospheric water vapour is located in the bottom-most few km with a certain degree of variability depending on season, latitude and atmospheric conditions. A typical humidity profile for Camborne for July 2009 is shown in Fig. 1.2.

Due to its high variability, both temporally and spatially, water vapour is one of the most difficult quantities to predict with numerical weather prediction (NWP) models. Typically, NWP model fields are initialised using existing model data coupled with observational data. Historically, observations of water vapour were relatively scarce in meteorology with the majority of data obtained from geographically and temporally sparse radiosonde ascents. Given that approximately half of the energy in the atmosphere is transported by water vapour, other parameters such as

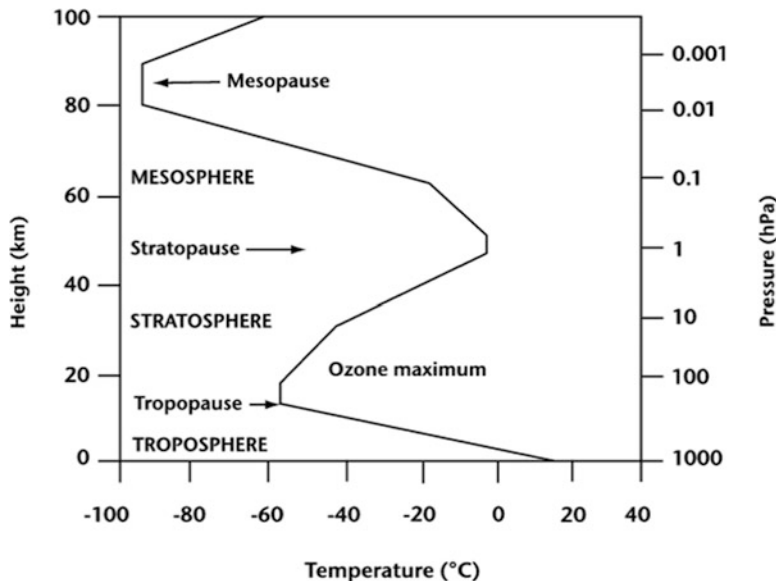


Fig. 1.1 Typical atmospheric temperature profile

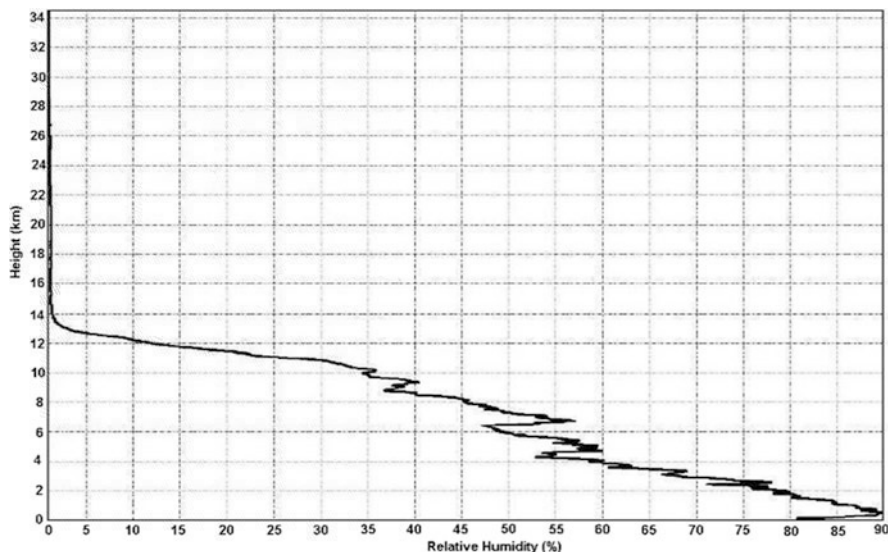
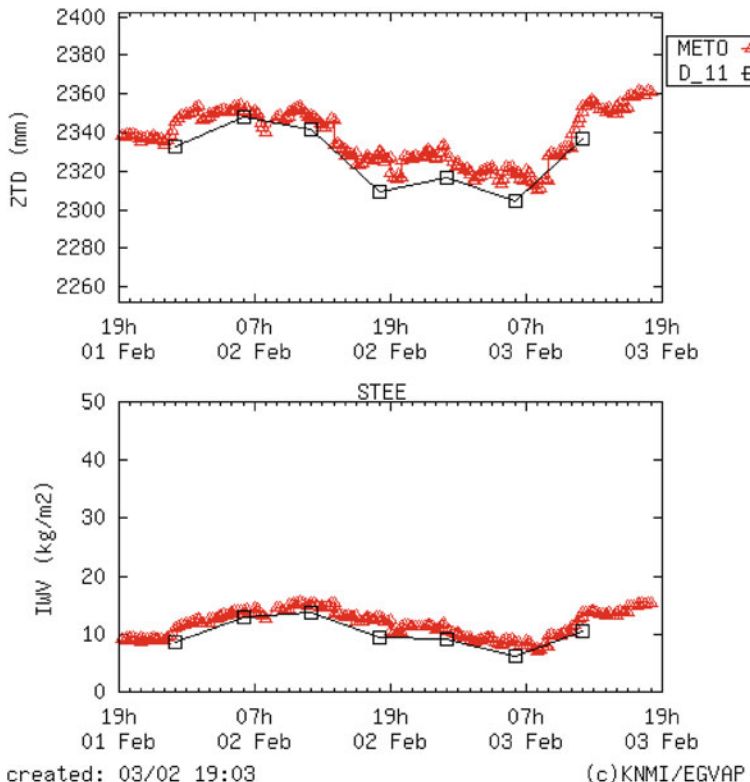


Fig. 1.2 Average monthly humidity profile, Camborne, UK. Composite of all RS92 operational radiosonde ascents from July 2009. (Courtesy of UK Met Office)



**Fig. 1.3** Time series of ZTD and IWV (for Stevenage, UK, February 2010) illustrating the divergence of a NWP model which does not assimilate GNSS observations from reality

cloud cover and surface temperature are also better forecast with superior water vapour information. Due to the importance of water vapour in operational meteorology, improved knowledge and understanding of water vapour fields is one of the prime focuses for future observing systems and is key to improving future forecasting capability.

Figure 1.3 represents a time series of GPS ZTD and IWV estimates from the UK Met Office GNSS system (METO) compared against the HIRLAM 11 km unified NWP model (Uden et al. 2002) prior to the HIRLAM model assimilating GNSS ZTD observations.

In the future, added computing power will permit NWP models with ever increasing horizontal, vertical and temporal resolution. As such, with the advent of higher resolution NWP models will come the requirement for ever higher resolution observational data to initialise the models' starting conditions.

Besides the importance of accurate water vapour observations to operational meteorology, water vapour is one of the most important controlling factors in mean atmospheric temperature by the absorption of radiation. Life on Earth is very much dependent on what is commonly referred to as the greenhouse effect. In general terms, this effect is generally the absorption of solar radiation in the atmosphere, which maintains the Earth's atmosphere at a habitable temperature in which life can exist. Earth has an average temperature of around 14 °C whereas if it were not for the presence of gases such as water vapour and carbon dioxide in the atmosphere, the Earth would have a mean atmospheric temperature of around -18 °C and life would not be possible as we know it.

Water Vapour is one of the most crucial greenhouse gases and plays a vital role in the global climate system. This role is not only restricted to absorbing and radiating energy from the sun, but has direct effects on the formation of clouds and aerosols and also of the chemistry of the lower atmosphere. Despite its importance to atmospheric processes over a wide range of spatial and temporal scales, water vapour is one of the least understood and poorly described components of the Earth's atmosphere in current climate prediction models. Atmospheric water vapour allows short wavelength radiation to pass through the atmosphere, but absorbs long wavelength radiation emitted back by the Earth's surface. This trapped radiation causes the temperatures to increase.

A systematic increase in air temperature due to increasing levels of greenhouse gases, such as CO<sub>2</sub> and methane, enables the air to contain more water vapour. In addition, evaporation will increase where water is available (from oceans, lakes, plants, soil etc). The increase in water vapour levels leads itself to additional absorption of radiation in the lower atmosphere, but also leads to changes in the amount of cloud formation, precipitation, reflection of sunlight from cloud tops etc. Thus, water vapour is generally thought of as a feedback rather than a cause of global warming. Even so, water vapour's role in the climate system is still not very well understood. In many climate models, details in the representation of clouds can substantially affect the model estimates of cloud feedback and climate sensitivity (e.g., Senior and Mitchell 1993; Stainforth et al. 2005; Yokohata et al. 2005). Moreover, the spread of climate sensitivity estimates among current models arises primarily from inter-model differences in cloud feedbacks (Colman 2003; Soden and Held 2006; Webb et al. 2006) and as such, water vapour and it's attributable cloud feedbacks remain a large source of uncertainty in climate sensitivity estimates.

With the advent of high precision ground based geodetic GNSS networks and high quality GNSS processing schemes, we now have a novel approach for the long term monitoring of atmospheric water vapour. GNSS networks are increasing in their global coverage and if the data can be used for climate applications, they offer a huge resource in terms of monitoring atmospheric water vapour long-term. Furthermore, due to the instruments' stability, high level of reliability and low level of maintenance, GNSS sensors are especially suited to remote regions of the world which are typically data sparse. The applicability of GNSS as a tool for climate applications is discussed further in Chap. 5.

## 1.2 Global Navigation Satellite Systems (GNSS)

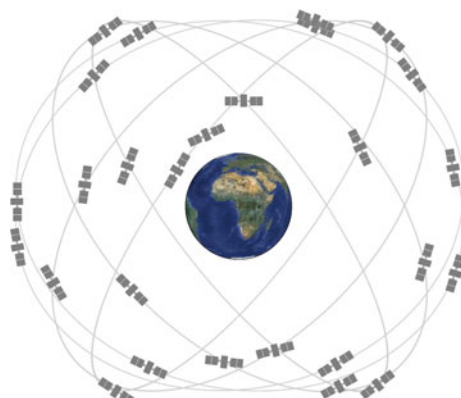
TRANSIT, was the first operational satellite navigation system. The system was developed to provide accurate location information to ballistic missile submarines. The system was rolled out for military use in January 1964 and subsequently to civilian users in July 1967. The system, using a constellation of five polar orbiting satellites in low Earth orbit (1075 km) was comprised of two carrier frequencies (150 and 400 MHz) which could be used to provide an hourly positioning estimate with an accuracy of between 200 and 400 m.

However, it wasn't until 1993 when the Global Positioning System (GPS) achieved operational capability that continuous three dimensional positioning and timing information became widely available allowing positioning accuracy down to the sub-decimetre level. The basic principle of GPS is that coded signals are transmitted by at least four satellites for the three dimensional position, plus the time element, to be determined. More information on the technique is given in the subsection below focusing on GPS basics. Whilst other GNSS systems are of course available and operational, the focus here is on GPS only - all other GNSS systems use the same basic principles (Fig. 1.4).

### 1.2.1 GPS Basics

All GNSS consist of three primary segments: space, ground and user. The space segment consists of satellites orbiting at an altitude of (in the case of GPS) approximately 20,200 km in orbital planes of 55 degrees to the equator. There must be at least 24 satellites operational to ensure at least 4 satellites are visible at any point on the Earth's surface, at any one time. The satellites transmit coded signals and other information (orbital parameters, satellite clock errors etc.) to the user. The ground segment consists of a master control station (in Colorado, USA for the GPS), as well

**Fig. 1.4** Representation of a GNSS satellite constellation



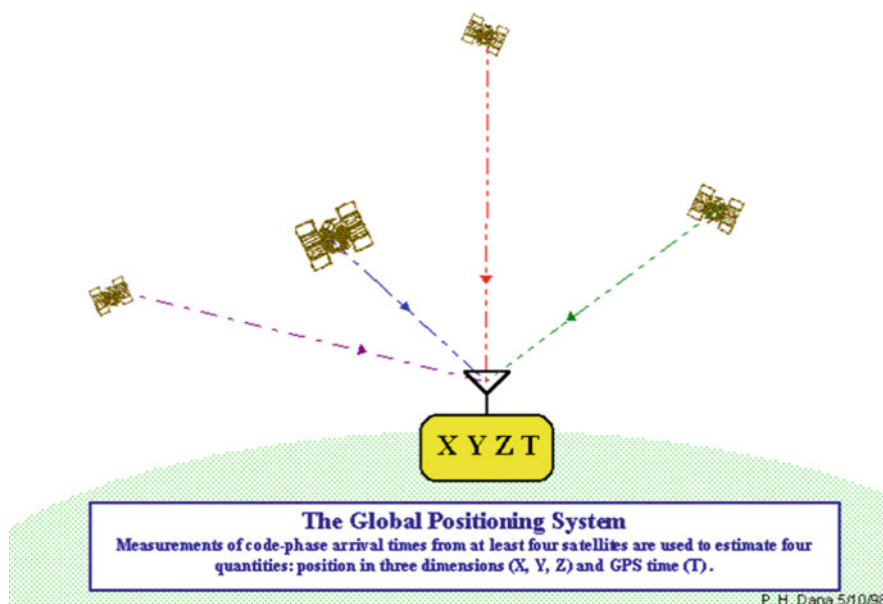


**Fig. 1.5** Illustration of GPS positioning

as a number of global monitoring stations, which are responsible for estimating essential satellite information such as orbits and clock errors.

On each GPS satellite, an onboard satellite oscillator generates the fundamental frequency ( $f_0$ ) of 10.23 MHz from which all other GPS signals are derived. Until relatively recently only two GPS sinusoidal carrier frequencies  $f_1$  and  $f_2$  (at 1575.42 MHz and 1227.60 MHz respectively) were generated which are right-hand polarized with respect to each other and are modulated with coded information. There are three codes imposed on the signal, the C/A (Coarse Acquisition or Clear-Access) code, the P (Precise or Protected) code and the navigation message. These codes have two states, a +1 or -1 state. As such if the phase-modulated L1 and L2 codes can be decoded by a ground based GPS receiver (the user segment) they may give the user positioning and velocity information, as summarised in Fig. 1.5. In recent times, additional GPS frequencies are transmitted such as L5 and L2C, however, the fundamentals of how the system is operated and it's application to meteorology is still largely based around the original two GPS frequencies.

The C/A code has a code sequence of 1023 bits in length and is transmitted with a frequency of 1.023 MHz. As such, it repeats itself once every millisecond and assuming the signal is travelling at the speed of light the distance between subsequent chips can be estimated to be  $\sim 300$  m. The generation of the P-Code is very similar with the length of the code sequence being approximately  $2.3547 \times 10^{14}$  bits which corresponds to a time span of approximately 266 days. The P-Code repeats itself once every week and through a process known as anti-spoofing (AS), the P-code is encrypted to a Y-code.

After signals are received by a GPS receiver, the signals are initially split into their satellite specific pseudorandom noise or PRN number based on the C/A codes. A carrier reference code is generated by the GPS receiver, modulated with a copy of the satellite specific PRN code and time shifted to compare against the received code. If the receiver and satellite clock errors are ignored, this difference gives the travel time ( $\tau$ ) and when multiplied by the speed of light (c) gives the approximate range or pseudo-range to the satellite.

Phase positioning measurements are based on reconstructing the carrier phase of the signal and comparing against a signal copy generated by the GPS receiver. By observing the difference in the phase of the signals transmitted by the GPS satellite and those stored in the GPS receiver, the phase difference may be obtained which can be resolved to provide the user with a distance measurement. This expression may be written as:

$$\Delta\phi = \phi_{obs} - \phi_{rec} \quad (1.1)$$

Positioning using phase differencing has a much higher accuracy, although it does introduce an integer ambiguity ( $j_{amb}$ ) which must be solved for. Furthermore additional delays in the signal propagation such as ionospheric delay ( $\Delta L_{ion}$ ), tropospheric delay ( $\Delta L_{trp}$ ) and clock differences between the satellite and receiver ( $\tau_{sat} - \tau_{rec}$ ) must all be accounted for if precise, geodetic positioning is to be achieved. From Blewitt (1997) the pseudorange, multiplied by the frequency,  $\lambda$ , may be expressed as:

$$\lambda\Delta\phi = D + c(\tau_{sat} - \tau_{rec}) - \lambda j_{amb} + \Delta L_{trp} + \Delta L_{ion} + E \quad (1.2)$$

Where D is the geometric range from receiver to satellite, c is the speed of light and E is the unknown errors such as receiver multipath. As there are more unknown parameters in Eq. 1.2 than known parameters, equations for a number of satellites are required if all parameters are to be solved for. Furthermore, satellite orbit and clock information must be known a-priori which can be obtained from the International GNSS Service (IGS), which is a voluntary federation of more than 200 worldwide organisations generating and providing free-of-charge GNSS products and services. With particular reference to this report, the IGS are essential in providing satellite clock corrections as well as both predicted and past satellite orbit information.

Even though the clock files provided by the IGS are of high quality there still remain clock errors in both satellite and receiver as well as un-calibrated phase errors which must be accounted for. These errors are common to all receivers and satellites and they can be eliminated by observing a number of satellites and receivers and forming what are known as baselines. Single difference baselines are formed by observing the same satellite by two receivers, in this way the satellite clocks and phase errors can be eliminated. By observing two satellites by two receivers the satellite clock, receiver clock and phase errors are all eliminated. However,

tropospheric errors can only be ignored if the baselines are relatively small and the stations are at roughly the same altitude, as the effect from the atmosphere will affect all signals in the same way.

The alternative to forming baselines between receivers to remove the clock errors, is to resolve the clock errors a-priori and thus introduce very accurate clock files into the processing in the first place. If this can be achieved, a network of GPS receivers can be processed in a station specific way, which is commonly referred to as Precise Point Positioning or PPP. The main benefits of PPP are that it is, at least for the coordinate and tropospheric estimation part, faster because the sites can be processed individually and the processing load can be shared over a number of CPUs/servers. Also, as the sites are processed individually, there is no risk of correlated errors as could be the case with the network solution. In reality however, any benefits in processing speed are often offset against the time it takes to generate the higher accuracy clocks and as such, the overall processing time for a national scale (approximately 200-receiver) network is often comparable to that taken by a double difference (DD) solution. It is when processing larger GNSS networks (300+ stations) where PPP typically has a speed advantage over DD. Furthermore, while a PPP system might not have any correlated errors between different parts of the network due to baselines, if any errors are introduced in the satellite clock determination part, those errors will be applied to the whole network being processed. For more information on the PPP method, see Kouba and Heroux (2001).

### 1.2.2 *Delay in the Neutral Atmosphere*

Once enough data has been collected from a number of satellites over a long enough time period, estimates can be generated of atmospheric delay as well as satellite clock errors and phase ambiguities. Due to the dispersive nature of the ionosphere it affects both GPS signals in the same way, by a mathematical combination of the L1 and L2 signals, a so-called ionosphere-free linear combination (L3) can be obtained and thus first order ionospheric delays can be eliminated. Second order effects are still present but their order of magnitude is so small they can be largely ignored for the purposes of this report.

$$L_3 = \frac{f_1^2}{f_1^2 - f_2^2} L_1 - \frac{f_2^2}{f_1^2 - f_2^2} L_2 \quad (1.3)$$

The atmosphere local to the GPS receiver is typically assumed to be horizontally homogenous and based on this assumption, slant path delays can be mapped into the vertical and the number of unknowns can be reduced further. While there is not enough power in the least squares adjustment to solve for slant paths directly, slant path delays are research topics at a number of atmospheric and geodetic institutes, but use of a-priori atmospheric model information is often necessary (Fig. 1.6). More

## Ionosphere

Electromagnetic signal propagation depends on the refractivity of medium

Dispersive, use dual GPS frequencies to resolve

Neutral Atmosphere

Non dispersive (troposphere + stratosphere)

- Using the Dry Neill mapping function: we can convert the slant path delays into a Zenith Total Delay (ZTD)

- Tropospheric path delay is due to many factors (dry atm. aerosols etc as well as the wet atm.)

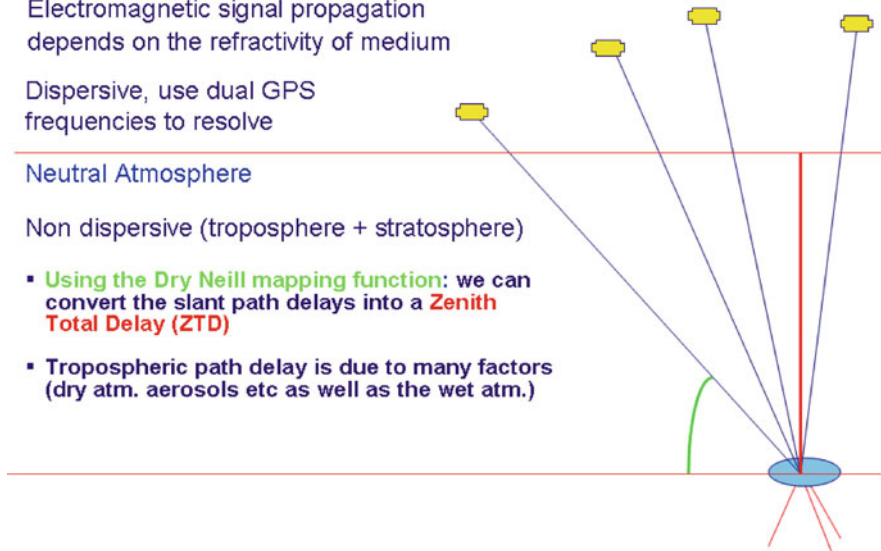


**Fig. 1.6** Schematic of satellite signal path through atmosphere

information on slant delays and tomographic retrieval can be found in Chap. 3 of this report.

Tropospheric delay can be expressed as:

$$\Delta^T = \int_s n ds - \int_g dg \quad (1.4)$$

where  $n$  is the refractive index,  $s$  is the actual signal path and  $g$  is the hypothetical geometric path. It is possible to rewrite this as:

$$\Delta^T = \int_s (n - 1) ds + \left( \int_s ds - \int_g dg \right) \quad (1.5)$$

This expression shows us that tropospheric delay is a combination of the excess geometric path length as well as the slowing of the signal propagation speed.

Excess geometric path length caused by changes in refractive index,  $n$ , is only of relevance at very high zenith angles where the signal is effectively being bent by the atmosphere and a bending angle is introduced. At the vast majority of satellite zenith angles, bending and thus excess path length is very small when compared to the delay of the signal due to propagation. From McClatchey et al. (1971) geometric delay at a zenith angle of  $80^\circ$  would only be in the region of  $\sim 4$  cm whereas at lower zenith angles (i.e. higher elevation angles) the delay due to slowing of the signal contributes to around 99.7% of the atmospheric delay. In current practice, most GPS